Journal of Magnetism and Magnetic Materials 408 (2016) 18–25

Contents lists available at ScienceDirect

Journal of Magnetism and Magnetic Materials

journal homepage: www.elsevier.com/locate/jmmm

Particle size dependent rheological property in magnetic fluid

Jie Wu, Lei Pei, Shouhu Xuan *, Qifan Yan, Xinglong Gong **

CAS Key Laboratory of Mechanical Behavior and Design of Materials, Department of Modern Mechanics, University of Science and Technological of China, Hefei 230027, People's Republic of China

ARTICLE INFO

Article history:
Received 21 December 2015
Received in revised form
1 February 2016
Accepted 4 February 2016
Available online 9 February 2016

Keywords:
Fe_3O_4 nanospheres
MRF
MR effects
Particle size
Shear stress
Viscosity

ABSTRACT

The influence of the particle size on the rheological property of magnetic fluid was studied both by the experimental and computer simulation methods. Firstly, the magnetic fluids were prepared by dispersing Fe_3O_4 nanospheres with size varied from 40 nm to 100 nm and 200 nm in the solution. Then, the rheological properties were investigated and it was found that the relative magnetorheological effects increased with increasing the particle size. Finally, the molecular dynamic simulation was used to analyze the mechanical characteristics of the magnetic fluid and the chain-like model agreed well with the experimental result. The authentic chain-like structure observed by a microscope agreed with the simulation results. The three particles composed of the similar cluster nanostructure, thus they exhibited similar magnetic property. To this end, the unique assembling microstructures was the origination of the mechanical difference. And it was found that the higher MR (magnetorheological) effects of the large particle based magnetic fluid was originated from the stronger assembling microstructure under the applying magnetic field.

1. Introduction

Magnetic fluids are a kind of smart materials which are prepared by dispersing the magnetic particles into the carrying fluids. Because of the magnetic dipolar–dipolar interaction among the magnetic particles, the magnetic fluids possessed typical MR effects, of which the viscosity could change reversibly and rapidly by tuning the external magnetic field [1–3]. According to the dispersing particles, the magnetic fluids could be simply divided into magnetorheological (MR) fluid and ferrofluid [4]. The magnetic saturation of the carbonyl iron particles is larger than the micro/nano-sized iron oxide, therefore, the relative MR effect in the MR fluid is higher than the ferrofluid. Due to their unique magnetic properties, the magnetic fluids have been attractive in a diverse range of applications, such as vacuum sealing, [5] magnetic resonance imaging, [6] intelligent sensors, [7] buffer solution in chips, [8,9] and drug delivery [10].

It is widely accepted that MR effect originates from the disorder to order transition of the particulate assembling under applying an external magnetic field [11]. Therefore, the magnetic property, shape, size, and inner-structure of the magnetic particles become the critical roles for affecting the rheological properties [12–15]. During the past decade, several groups performed intensive work in this area to investigate the MR mechanism. Magnetic particles with various morphologies such as the cubic, [16] octahedral, [17,18] rod, [19,20] fiber [21] were applied for preparing MR fluids. Stronger assembling chains would be obtained for the anisotropic magnetic particles than the spherical ones, [22] because they have a larger contact surface. The larger friction force among the aggregated particles led to the higher viscosity. Moreover, the recent research indicated that the bundle wire-like aggregations composed of magnetic wires were more stable than the magnetic particles, thus wires based magnetic fluid presented better MR effect than the one composed of monodisperse particles [23]. To this end, the investigation of the particle structure dependent MR effects is favorable.

How does the particle size influence the mechanical properties of the magnetic fluid? This is a very fundamental question for understanding the MR mechanism [24]. Unfortunately, few work has been reported on this subject. The mostly used magnetic particles in MRF is commercial carbonyl iron, whose size is only tunable between several um to tens of um. If the size of the iron particles decreases to nano sized, they are very un-stable [25]. Therefore, other particles with tunable sizes are expected to solve this problem. Recently, Fe_3O_4 based magnetic fluids have attracted increasing interests since their better stability than the common carbonyl iron based MR fluid [26–29]. The magnetization of the Fe_3O_4 micro/nanospheres is sufficient for usage thus they could be considered as a proper substitution in MR materials. Various preparation method for Fe_3O_4 micro/nanospheres were reported and the size, shape, magnetic property of the Fe_3O_4 could be

* Corresponding author.
** Corresponding author.
E-mail addresses: xuansh@ustc.edu.cn (S. Xuan), gongxl@ustc.edu.cn (X. Gong).

http://dx.doi.org/10.1016/j.jmmm.2016.02.005
0304-8853/

targetingly obtained [30–33]. Therefore, the Fe_3O_4 is not only an ideal candidate for understanding the MR mechanism but also attracting for its application.

In this work, the influence of the particle size on the rheological properties of the Fe_3O_4 magnetic fluids was both experimentally and theoretically studied. Firstly, the Fe_3O_4 nanospheres with different size were synthesized by using a modified solvothermal method [34]. Then, the rheological property of the Fe_3O_4 magnetic fluids thereof was tested and it was found that the MR effects increased with the particle size. Finally, the molecular dynamic simulation was used to analyze the mechanical characteristics of the magnetic fluid. The proposed chain-like model agreed well with the experimental result. This work is valuable for further understanding the origination of the MR effect.

2. Experimental

2.1. Chemicals

Diethylene glycol (DEG), ethylene glycol (EG), and polyacrylic acid (PAA) were purchased from Sigma-Aldrich. Iron(III)chloride hexahydrate ($FeCl_3 \cdot 6H_2O$) and sodium acetate anhydrous (CH_3COONa, NaAC) were obtained from Sinopharm Chemical Reagent Co., Ltd. All chemicals were of analytical grade and used without further purification. Deionized water was used in these experiments.

2.2. Preparation of magnetic fluids with different Fe_3O_4 particle sizes

Monodisperse Fe_3O_4 nanospheres with different sizes were synthesized in a binary solvent system with diethylene glycol (DEG) and ethylene glycol (EG). Typically, $FeCl_3 \cdot 6H_2O$ (2.16 g), NaAC (8 g) and PAA (0.2 g) were dissolved in an 80 mL mixture of DEG and EG. After stirring for 30 min, the obtained yellow solution was transferred into a telfton-lined stainless-steel autoclave. The sealed reactor was heating at a temperature of 200 °C for 12 h. By cooling to room temperature, the obtained Fe_3O_4 nanospheres were washed by ethanol and deionized water for 5 times, respectively. Finally, about 0.6 g Fe_3O_4 nanospheres were achieved under drying in a vacuum oven. Here, the size of the Fe_3O_4 nanospheres was tunable by varying the DEG/EG ratio. The ratio of 64/16 leads to 40 nm, while the 60/20 and 50/30 leads to 100 and 200 nm, respectively. The relative Fe_3O_4 nanospheres based MRFs were prepared by dispersing the above powder into the carrying fluid. Thus the relative MRFs prepared by 40, 100, 200 nm nanospheres were defined as MRF-40, MRF-100 and MRF-200, respectively.

2.3. Characterization

The transmission electron microscopy (TEM) images were obtained on a JEM-2100F at an accelerating voltage of 200 kV. The samples which were diluted in absolute ethyl alcohol were deposited on a double-sided copper grid for TEM observation. X-ray diffraction (XRD) patterns of the samples were obtained with a Japan RigakuDMax-γA rotating anode X-ray diffraction equipped with graphite with graphite monochromatized Cu Kα radiation ($\lambda = 1.54178$ Å). Infrared (IR) spectra in the wavenumber range 4000–400 cm^{-1} were recorded with a TENSOR Model 27 Fourier transition infrared (FT-IR) spectrometer using a KBr wafer. Thermogravimetric (TG) analysis was conducted on a DTG-60 H thermogravimetric instrument, samples were analyzed in alumina pans at a heating rate of 10 °C min^{-1} to 700 °C under the atmosphere of air flowing at 50 mL min^{-1}. The Au contents of the products were determined on an Optima 7300DV inductive coupled plasma atomic emission spectrometer (ICP-AES). The UV–vis spectra were records on a TU-1901 spectrophotometer. A magnetic property measuring system (MPMS) vibrating sample magnetometer (VSM) (SQUID, Quantum Design Co., America) was used in studying the magnetic hysteresis loops of Fe_3O_4 nanospheres with different diameters.

2.4. Rheological properties of the magnetic fluid

The rheological properties of the Fe_3O_4 nanospheres based MRFs were investigated by using a commercial rheometer (Physica MCR 301, Anton Paar Co., Austria) with a magnetic field generator. 1 mL of the testing sample was placed on the plate in a uniform magnetic field. The magnetic field was applied perpendicular to the double parallel plates of the rheometer, thus the obtained particle chains were also perpendicular to the flow direction. The gap between the plates was kept at 1 mm. There were two types of measurements: magnetic flux density sweep tests and shear rate sweep tests. Pre-shearing and pre-structuring were carried out before the rheological tests. For the magnetic flux density sweep, the shear rate was set as 10 s^{-1}, 50 s^{-1}, 100 s^{-1}, 200 s^{-1} while the magnetic field density was varied from 0 mT to 160 mT at room temperature. On the other hand, the rheological curves were also obtained in shear rate sweep tests by changing the shear rate, while keeping the magnetic flux density as a constant.

3. Results and discussion

3.1. Characterization of Fe_3O_4 nanospheres with different sizes

In this work, the Fe_3O_4 nanospheres were synthesized by a modified bi-solvent solvothermal method. By varying the ratio of DEG/EG, the size of the Fe_3O_4 nanospheres was tunable. When the ratio was 64/16, 40 nm Fe_3O_4 nanospheres. As shown in Fig. 1, all the obtained Fe_3O_4 nanospheres was well dispersed without aggregations. Typically, these Fe_3O_4 nanospheres were composed of large amount of tiny nanocrystals, thus presented a cluster-like nanostructure, which agreed well with the previous report. The 100 nm and 200 nm Fe_3O_4 nanospheres also exhibited the similar secondary nanostructure. The Fe_3O_4 nanospheres have uniform spherical shape and size with narrow distribution enable them to be ideal candidate for preparing the MRF.

Fig. 2(a) showed the XRD diffraction pattern of the Fe_3O_4 nanospheres with 100 nm. The strong peaks in the pattern could be indexed to be the (220), (311), (400), (422), (511) and (440) crystal face in the cubic Fe_3O_4 (19-0629). No other peak was found in the XRD pattern, indicating the purity of the final product. Moreover, the broad nature of the peak also indicated the Fe_3O_4 nanospheres consisted of small nanograins, which agreed the TEM analysis. Here, the polyacrylic acid was used as the surfactant during the synthesis, thus it inevitably presented in the final nanospheres. Fig. 2(b) presented the typical FTIR spectrum of the Fe_3O_4 nanospheres. The two peaks located at 1550 and 1405 cm^{-1} were corresponded to the COO^- antisymmetrical vibration and COO^- symmetric vibration, indicated that large amounts of carbonxylate groups were strongly coordinated to the iron cations [35]. Due to the presence of this water-soluble polymer, the as prepared Fe_3O_4 nanospheres could be dispersed into the water to form stable dispersion. The TG curve demonstrated that there was a large weigh loss between 200–300 °C in Fig. 2(c), which may be attributed to the residue PAA content in the Fe_3O_4 nanospheres. By calculation, the weight ratio of the PAA was about 10%.

The magnetic properties of the Fe_3O_4 nanospheres with different diameters were investigated by a MPMS VSM at room temperature. Fig. 3 shows the hysteresis loops of the samples. All

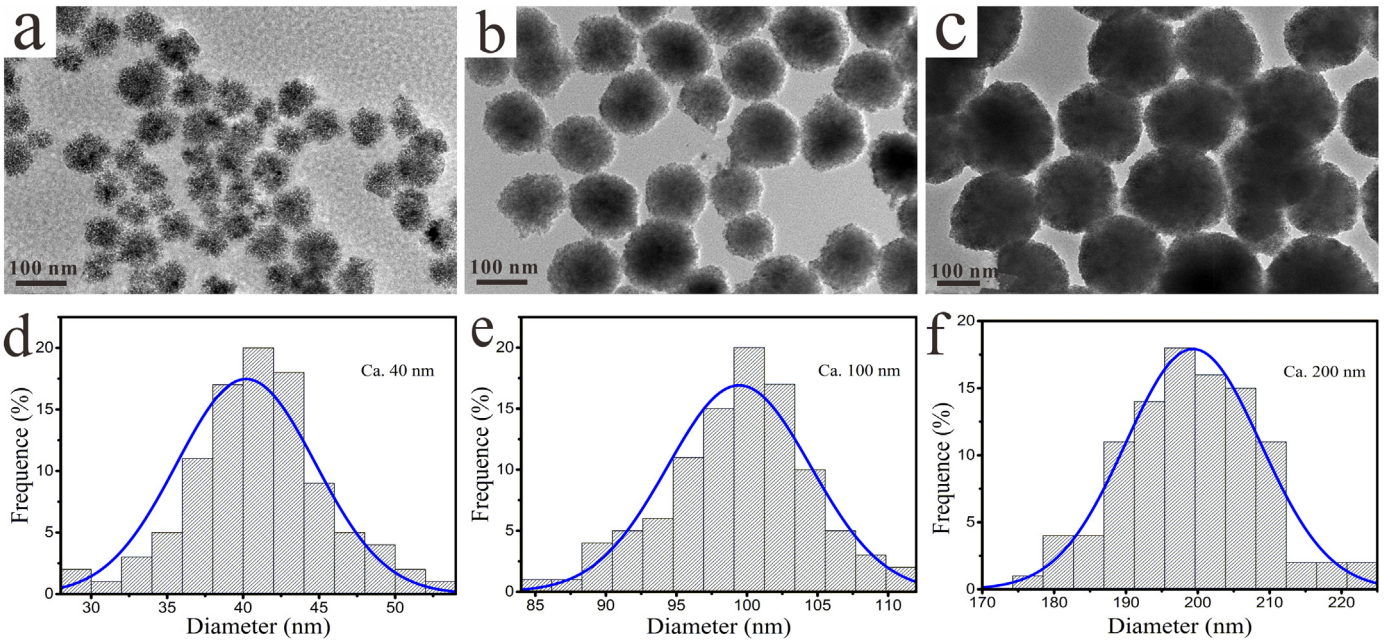

Fig. 1. TEM images of the obtained Fe_3O_4 nanospheres with average diameters of (a) 40 nm, (b) 100 nm, (c) 200 nm. Histograms of particle sizes distribution of the obtained Fe_3O_4 nanospheres with average diameters of (d) 40 nm, (e) 100 nm, (f) 200 nm.

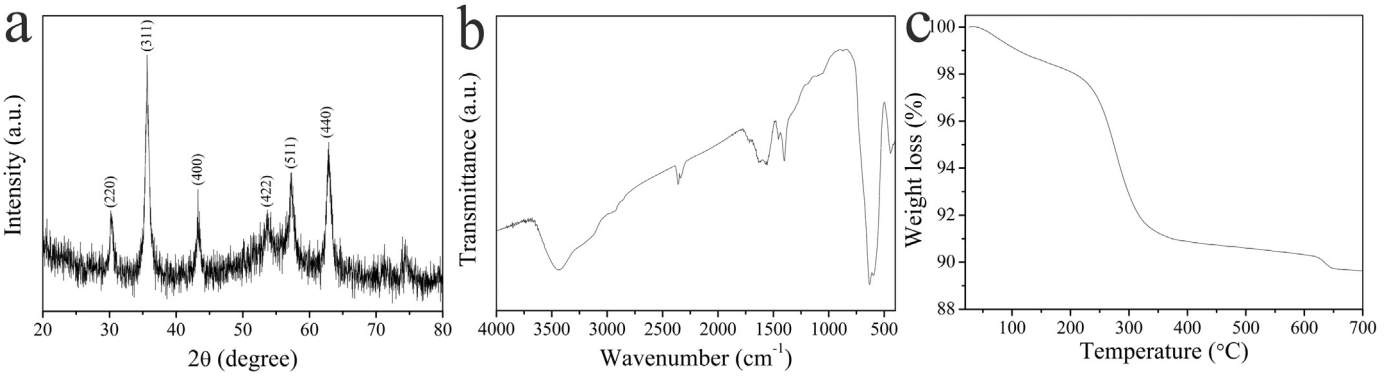

Fig. 2. (a) XRD pattern of the obtained Fe_3O_4 nanospheres. (b) FTIR pattern of the obtained Fe_3O_4 nanospheres. (c) TG curve of the obtained Fe_3O_4 nanospheres.

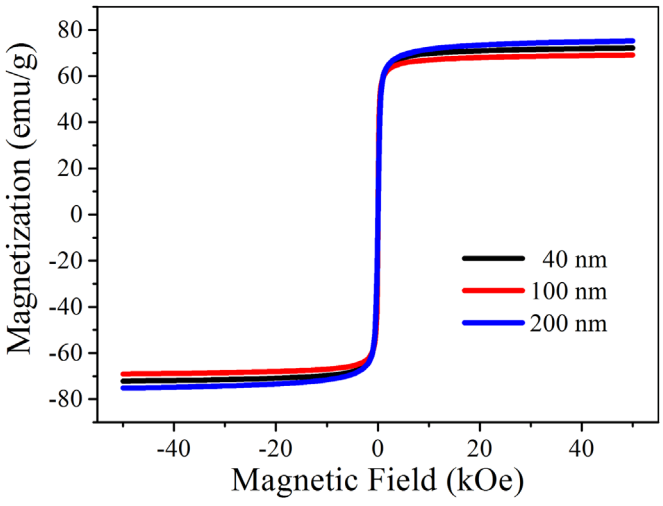

Fig. 3. The magnetic hysteresis loops (magnetization versus an applied magnetic field) of Fe_3O_4 nanospheres with different diameters.

the hysteresis loops are smooth and no hysteresis was found which indicated the coercive force and the residual magnetization approach to zero. Clearly, all the Fe_3O_4 nanospheres exhibited superparamagnetic behavior. Interestingly, the magnetic saturation of the Fe_3O_4 nanospheres with 40 nm, 100 nm, and 200 nm were 70, 68, 72 emu/g, respectively. The variation of the Ms is very small, which indicated the three kind of nanospheres showed almost the same magnetic property. The above analysis indicated that the Fe_3O_4 nanospheres exhibited a cluster-like nanostructure, thus the secondary nanograin played a critical role on the magnetic property. Although the size of the Fe_3O_4 nanospheres was different, they depicted similar secondary nanostructure. To this end, the magnetic characteristics of the Fe_3O_4 nanospheres with different size were almost the same.

3.2. Magneto-responsive rheological properties of the magnetic fluids based on different Fe_3O_4 sizes

The same magnetic property of the magnetic particle is the most important precondition for investigating the structure dependent

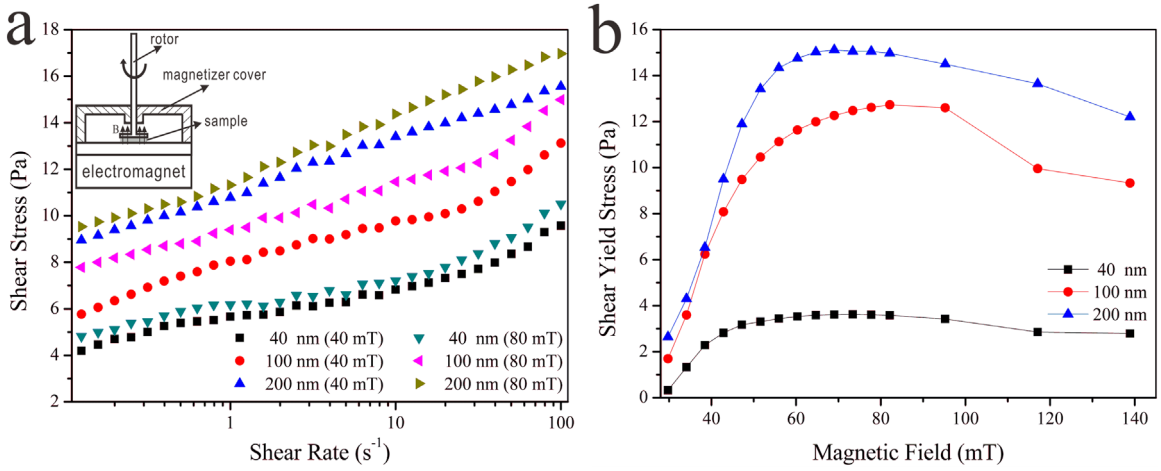

Fig. 4. (a) Shear stress as a function of shear rate, magnetic field intensity, particle sizes. (b) Shear yield stress as a function of magnetic field intensity and particle sizes. In this figure (a) the sketch of the Physica MCR301 test system. The weight ratio of the Fe_3O_4 in the magnetic fluid is 10%.

magnetic fluid. To our knowledge, the systematically studying the influence of the particle size on the rheological property of the MRF has not been conducted due to the difficulty of the preparation of magnetic particle with different size but the same magnetic property. In this work, the ideal candidate was obtained by the solvothermal method and the MRFs were prepared by dispersing the relative sized Fe_3O_4 nanospheres into deionized water, in which the mass fraction of the magnetic particles were kept at 10%.

Fig. 4(a) showed the typical shear rate dependent shear stress of the as prepared MRFs. Similar to the tradition MRFs, the shear stress increased with the shear rate under applying the constant magnetic field [36]. It was found that the shear stress was dependent on the size of the Fe_3O_4 nanospheres. Clearly, under the same shear rate, the MRF-200 showed higher shear stress than the MRF-100 and MRF-40. Moreover, the larger magnetic field often led to the higher shear stress. Fig. 4(b) showed the magnetic field dependent shear stress of the relative samples. Obviously, the shear stress increased with the magnetic field, demonstrated the typical MR effect. The quickly increment within 60 mT magnetic field indicated the quick saturation of the magnetic particles and

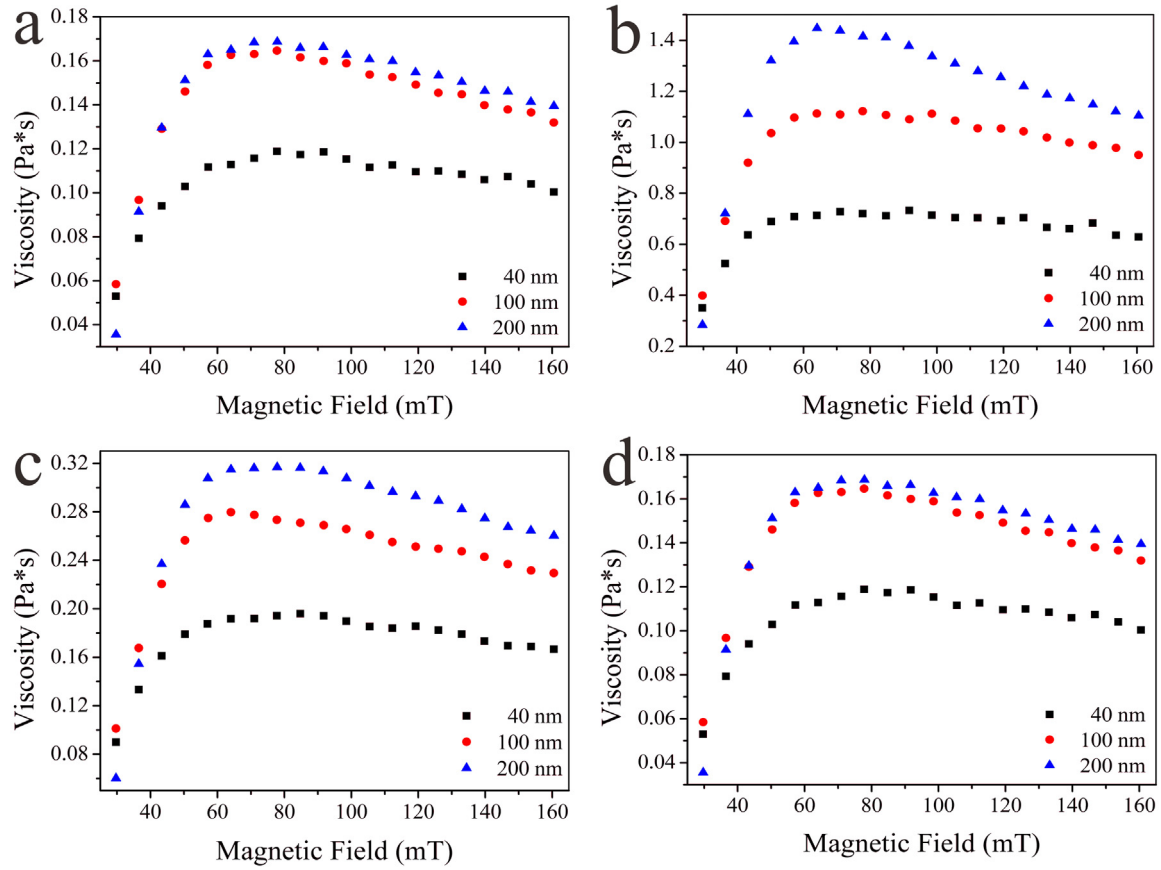

Fig. 5. (a) Viscosity versus magnetic field of MRFs with 100 nm Fe_3O_4 nanospheres at different shear rate. (b) Viscosity versus magnetic field of MRFs with three different sizes Fe_3O_4 nanospheres at a constant shear rate of 10 s^{-1}. (c) Viscosity versus magnetic field of MRFs with three different sizes Fe_3O_4 nanospheres at a constant shear rate of 50 s^{-1}. (d) Viscosity versus magnetic field of MRFs with three different sizes Fe_3O_4 nanospheres at a constant shear rate of 100 s^{-1}.

the level off must be attributed to its unique magnetic characteristics. The magnetic induced shear stress for the MRF-40, MRF-100 and MRF-200 were calculated to be 3.5, 11, and 12 Pa respectively. Therefore, the MR effect increased with increasing the particle size.

Under the applying magnetic field, the magnetic particles aligned in the magnetic direction to form chain-like structures. Since the increased dipole–dipole interaction, the viscosity of the MRF increased and presented the MR effect. In our measurement, the mass fraction was kept as a constant. With the increasing of the size, the total particle number in the fluid decreased while the volume fraction was not changed. In this case, stronger assembling chains may be formed in the MRF with large Fe_3O_4 nanospheres. Horia Chiriac claimed that the greater magnetostatic interaction would present between the larger magnetic particles. Therefore, the larger Fe_3O_4 nanospheres in the MRF led to the higher MR effect. Too larger magnetic particles led to much smaller particle number, thus the increment of the MR effect decreased with further increasing the particle size from 100 nm to 200 nm.

Fig. 5(a) showed the influence of the magnetic field on the viscosity of the MRF-100. Similar to the shear stress, the viscosity of MRF was firstly reached the highest value and then tend to level off. The shear rate showed an important effect on the viscosity and the increased shear rate led the decrement of the viscosity. Fig. 5 (b) showed the magnetic field dependent viscosity under the shear rate of 10 s^{-1}. It was found that the viscosity increased with the magnetic field and the MR effect increased with the particle size. Similar results were also obtained in the other two conditions (50 s^{-1} and 100 s^{-1}). Interestingly, with increasing of the shear rate, the difference of the curve for large particle based MRFs became reduced. As we know, the MR effect was origination from the transformation of uniform dispersion to ordered assembling of the magnetic particles. These chains structure must be destroyed by the shear and be re-assembled under the magnetic field. Under higher shear rate, the re-assembling would be weaker thus the viscosity decreased with increasing the shear rate. It means that the shear rate becomes high enough breaking the chains, which is faster than reforming the chains, then the MRF starts to flow. With increasing of the particle size, the increment of the particle–particle interaction decreased and the number of the assembling chains decreased, thus the difference of the viscosity decreased with increasing of the shear rate.

Mason number was also introduced to show the influence of magnetic field and shear rate on the MRFs with different particle size. Kniti Shah used the ratio between the hydrodynamic and magnetostatic forces acting on the particles as the Mason number (Mn) [37].

Here, $Mn=\frac{\eta_c\dot{\gamma}}{2\mu_0\mu_c\beta^2H^2}$, where η_c means the viscosity of continuous phase. $\mu_0=4\pi\times10^{-7}N\bullet A^{-2}$ is the permeability of free space, μ_c is the relative permeability of the continuous phase, and H is the applied magnetic field strength. $\beta=(\mu_p-\mu_c)/(\mu_p+2\mu_c)$, where μ_p is the relative permeability of the particle material. Here, it was assumed that $\mu_p\gg\mu_c$ and then $\beta\approx1$, thus the dimensionless viscosity as a function of Mason number of the magnetic fluid was plotted in Fig. 6 (the originated data was from Fig. 3). The Mason number showed an important effect on the dimensionless viscosity and the increased Mason number led the decrement of the dimensionless viscosity. The data can be fitted by a power law: $\frac{\eta_{app}}{\eta_{inf}}\propto M_n{}^{-k}$. And the power exponent, $k\approx0.75$, does not show any dependence to the magnetic field strength, particle size and shear rate.

3.3. Theoretical simulation of the structure transformation in the magnetic fluids with different Fe_3O_4 sizes

Albert P. Philipse and Dinia Mass have developed a chain model to describe the MR properties of MRF [38]. Under applying the magnetic field, soft chain-like structure was formed due to the dipole–dipole interaction. Since the chain-like structure, the viscosity of the MRF increased. If the shear rate is small, the chain-like structure is hard to be destroyed. However, when the shear rate is high, the structure will be destroyed easily and further lead to the decrement of the viscosity. The dipole interaction energy u_m between two neighboring particles can be described by this formula: [39]

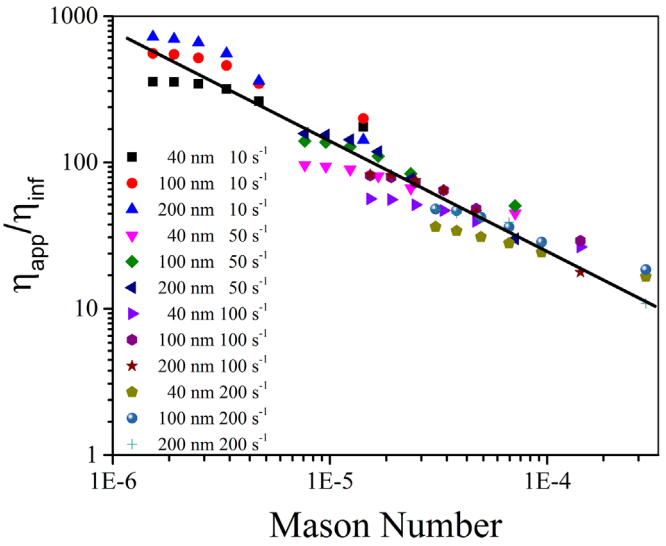

Fig. 6. Dimensionless viscosity versus the Mason Number of MRFs with three different sizes Fe_3O_4 at different shear rate. The line is a fit to a power law and the power exponent value is k=0. 75.

$$u_{ij}^m=\frac{\mu m_i^2}{4\pi d_p^3}\bullet\left(\frac{d_p}{r_{ij}}\right)^3(3\,cos^2\,\theta-1) \tag{1}$$

Here m_i means the magnetic moment of a particle, μ is the permeability, d_p the particle diameter, r_{ij} is the center-to-center distance between two neighboring particles and θ is the angle between the center-to-center vector and the magnetic field. The value of m was showed by Gans etc [40].

$$m_i=4\pi d_p^3\frac{MH}{2M+3H} \tag{2}$$

M denotes the magnetization of the MRF and H means the magnetic field. Fig. 3 showed the hysteresis loops of different sizes Fe_3O_4 nanospheres and the value of the magnetization were almost the same.

The influence of applied magnetic field also concludes:

$$F_i^h=\mu(m_i\bullet\nabla)H \tag{3}$$

Here F_i^h denotes magnetic field force to Fe_3O_4 nanoparticle.

Molecular dynamics simulations were preformed to analyze the MR effect. A cube, L in length, was considered in this model. Appreciable quantity Fe_3O_4 nanospheres which were dispersed in deionized water constituted this computing element. Only the dipole interaction energy u_{ij}^m between two neighboring particles and the external magnetic energy u_i^h to each particle were taken into account in this system. So the system energy could be described as:

$$U=u_{ij}^m+u_i^h \tag{4}$$

$$u_{ij}^m=\frac{\mu_0 m^2}{4\pi r_{ij}^3}\left[\boldsymbol{n}_i\bullet\boldsymbol{n}_j-3\left(\boldsymbol{n}_i\bullet\boldsymbol{t}_{ij}\right)\left(\boldsymbol{n}_j\bullet\boldsymbol{t}_{ij}\right)\right] \tag{5}$$

$$u_i^h = -\mu_0 mH\boldsymbol{n}_i \bullet \boldsymbol{h} \tag{6}$$

Here, i and j are the sequence number of those nanospheres. $\boldsymbol{m}_i$ means natural magnetic moment and $\boldsymbol{n}_i=\boldsymbol{m}_i/m_i$. Similarly, $\boldsymbol{H}$ means external magnetic field intensity and $\boldsymbol{h}=\boldsymbol{H}/H$, $\boldsymbol{r}_{ij}$ ($\boldsymbol{r}_{ij}=\boldsymbol{r}_i-\boldsymbol{r}_j$) is the relative positional vector and $\boldsymbol{t}_{ij}=\boldsymbol{r}_{ij}/r_{ij}$. Permeability of vacuum equals to $\mu_0=4\pi\times10^{-7}N\bullet A^{-2}$.

The gradient of the system energy can be used to express the stress state of each particle in the MRF.

$$\boldsymbol{F}_i = -\nabla_i U = -\left(\boldsymbol{i}\frac{\partial}{\partial x_i}+\boldsymbol{j}\frac{\partial}{\partial y_i}+\boldsymbol{k}\frac{\partial}{\partial z_i}\right)U \tag{7}$$

$$\boldsymbol{F}_{ij}^m = \lambda_m kT\frac{3d_p^3}{r_{ij}^4}\left\{-(\boldsymbol{n}_i\bullet\boldsymbol{n}_j)\boldsymbol{t}_{ij}+5(\boldsymbol{n}_i\bullet\boldsymbol{t}_{ij})(\boldsymbol{n}_j\bullet\boldsymbol{t}_{ij})\boldsymbol{t}_{ij}-\left[(\boldsymbol{n}_i\bullet\boldsymbol{t}_{ij})\boldsymbol{n}_j+(\boldsymbol{n}_j\bullet\boldsymbol{t}_{ij})\boldsymbol{n}_i\right]\right\} \tag{8}$$

$$\boldsymbol{F}_i^h = \mu_0(\boldsymbol{m}_i\bullet\nabla)\boldsymbol{H} \tag{9}$$

$$\boldsymbol{T}_{ij}^m = -\lambda_m kT\frac{3d_p^3}{r_{ij}^3}\left[\boldsymbol{n}_i\times\boldsymbol{n}_j-(\boldsymbol{n}_j\bullet\boldsymbol{t}_{ij})\boldsymbol{n}_i\times\boldsymbol{t}_{ij}\right] \tag{10}$$

$$\boldsymbol{T}_i^h = \mu_0 mH\boldsymbol{n}_i\times\boldsymbol{h} = \mu_0\boldsymbol{m}_i\times\boldsymbol{H} \tag{11}$$

$\boldsymbol{F}_{ij}^m$, $\boldsymbol{F}_i^h$, $\boldsymbol{T}_{ij}^m$ and $\boldsymbol{T}_i^h$ indicate particles' interaction force, external magnetic force, particles' interaction moment of force and external magnetic moment of force, respectively. Dimensionless parameter $\lambda_m=\frac{\mu_0 m^2}{4\pi d_p^3 kT}$, Boltzman constant $k=1.38\times10^{-23}J/K$. In addition, Brownian motion force is $\boldsymbol{F}_i^b=\sqrt{\frac{12\pi\eta_S akT}{\Delta t}}\boldsymbol{n}_b$.

Neither the inertia effect nor stochastic motion of the nanospheres was taken into account. There is no necessary to consider the magneto-induced body rotational motion of the particles because the Fe_3O_4 is superparamagnetic and the magnetic torque applied on the nanospheres is very weak. It can be concluded that the magnetic interaction of the particles dominates their random thermal motion when an external magnetic field is applied rapidly, which was discussed similarly for magnetorheological fluids by Mohebi [41]. Consulting Akira Satoh' work, [42] the kinematic equation can be constructed as:

$$\frac{d\boldsymbol{r}_i}{dt} = \dot{r}Z\hat{\boldsymbol{x}} + \frac{1}{\varsigma_t}\left(\sum_{j\neq i}\boldsymbol{F}_{ij}^m + \boldsymbol{F}_i^b\right) \tag{12}$$

$$\frac{d\boldsymbol{n}_i}{dt} = \left[\frac{\dot{\gamma}}{2}\hat{\boldsymbol{y}} + \frac{1}{\varsigma_r}\left(\sum_{j\neq i}\boldsymbol{T}_{ij}^m + \boldsymbol{T}_i^h\right)\right]\times\boldsymbol{n}_i \tag{13}$$

When solving the equations, nanospheres were dispersed in the MRF randomly and the initial velocity was set as zero. Euler formula was used to calculate these particles' motion equation.

$$\boldsymbol{r}_i(t_0+\Delta t_0) = \boldsymbol{r}_i t_0 + \frac{d\boldsymbol{r}_i}{dx}\Big|_{t=t_0}\Delta t_0 \tag{14}$$

$$\boldsymbol{n}_i(t_0+\Delta t_0) = \boldsymbol{n}_i t_0 + \frac{d\boldsymbol{n}_i}{dx}\Big|_{t=t_0}\Delta t_0 \tag{15}$$

Fig. 7 showed the system potential energy of each computing element. It was found that the element with lager size particles had a lager potential energy. Clearly, with increasing of the particles size, the magnetic potential energy of the MRF increased. The MRF-200 had the strongest chain-like structure when the external magnetic was applied.

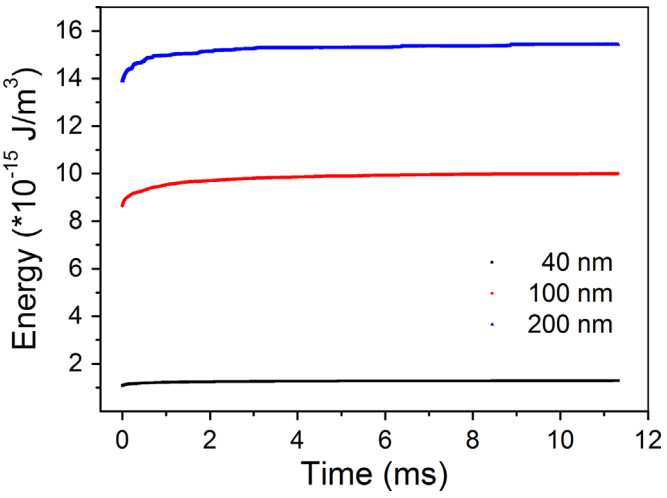

Fig. 7. Potential energy of the computing element versus time. An adaptive time step of order $\Delta t=0.001s$ is employed in all simulations.

Moreover, the inner-structure transformation also could obtained by using the molecule dynamic (MD) analysis. Fig. 8(a)–(c) shows the chain-like structure in the MRF motivated by external magnetic through the results from MD analysis. With increasing of particle sizes, the distance (r_{ij}) of every two neighboring particles decreased. As a result, particles' interaction force, external magnetic force, particles' interaction moment of force and external magnetic moment of force, which showed in Formula (8)–(11), would increase with increasing of nanoparticle sizes from 40 nm to 200 nm. Furthermore, the authentic chain-like structure was observed under a microscope by pumping the MRF with different size into a same microchip [43]. A permanent magnet was placed parallel to the main channel of the chip to provide the magnetic field. The particle chains in Fig. 8(d) were intensive and spindly and thicker in Fig. 8(e). Fig. 8(f) showed the most thickest and extraordinary sparse particle chains due to the largest particle size. It can be concluded that the simulation results showed the same tendency with the experimental observation by contrasting Fig. 8(d)–(f) with figure (a), (b) and (c). Therefore, the MRF with larger size particles showed much better magnetorheological properties. As a result, the strength of chain-like structure increases with the increasing of the nanospheres sizes (d_p) and the magnetic field strength (H). That is the reason that the viscosity and shear yield stress have a positive dependence to particle sizes and magnetic field. The simulation result agreed well with the experimental results.

4. Conclusions

In conclusion, a novel kind of magnetic fluids with tunable MR effects were developed. Firstly, the Fe_3O_4 nanospheres with controllable size were prepared by using a binary solvothermal method. Then, the rheological properties of the MRF thereof were investigated by both the experimental and simulation analysis. It was found that the relative magnetorheological effects increased with increasing the particle size. Due to the larger dipolar–dipolar interaction and the stronger chains structure, the MRFs with larger particle size gave the better MR effect. The chain-like model could well describe the MR mechanism and it matched well with the experimental result. This work supplied valuable information for further understanding the MR origination.

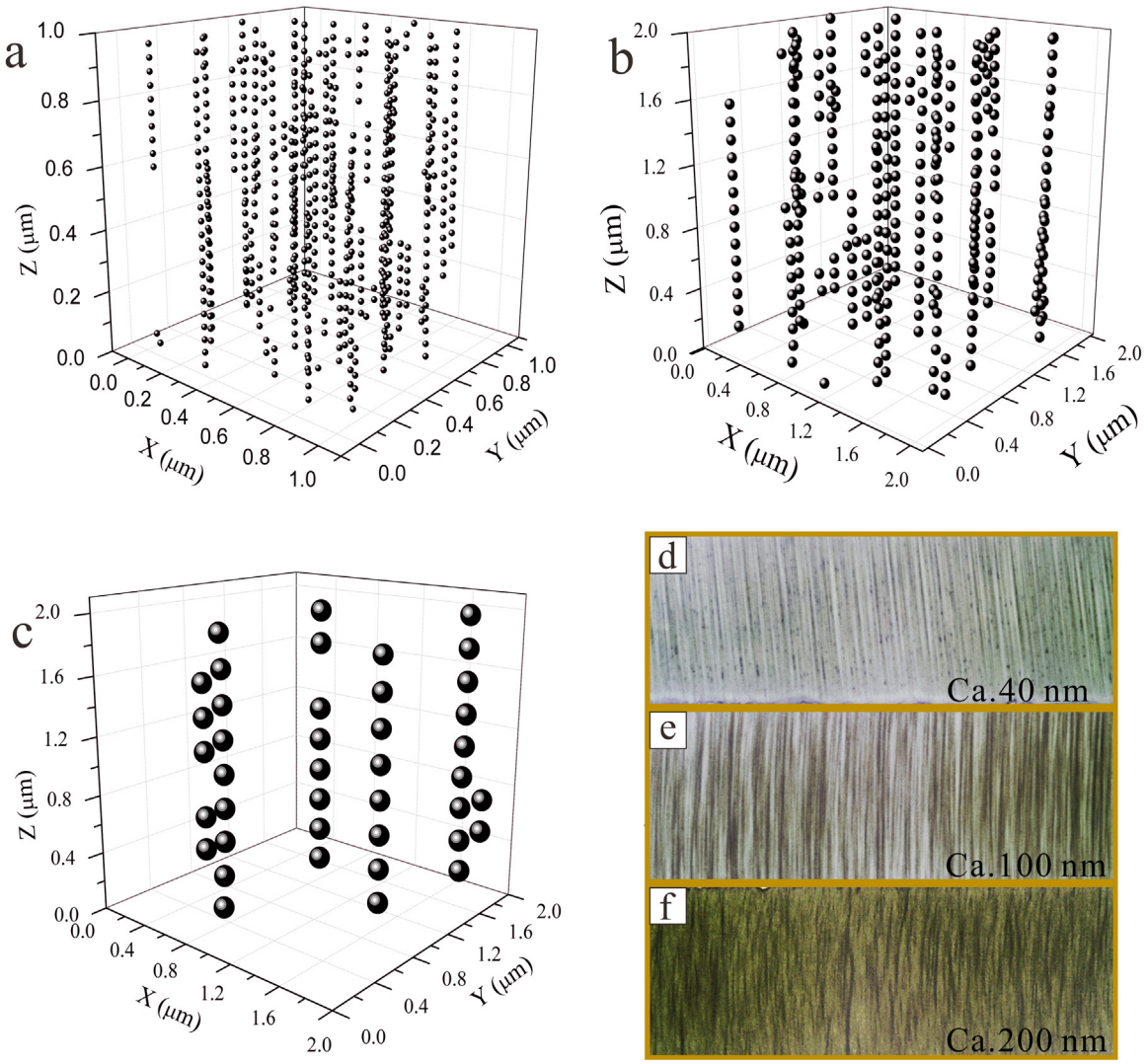

Fig. 8. (a) Microstructure of MRF with 40 nm Fe_3O_4 nanospheres, (b) Microstructure of MRF with 100 nm Fe_3O_4 nanospheres, and (c) Microstructure of MRF with 200 nm Fe_3O_4 nanospheres. The magnetic field intensity is 120 kA/m. (d) Chain-like structure of MRF with 40 nm Fe_3O_4 nanospheres, (e) Chain-like structure of MRF with 100 nm Fe_3O_4 nanospheres, (f) Chain-like structure of MRF with 200 nm Fe_3O_4 nanospheres.

Acknowledgment

This work was supported by Collaborative Innovation Center of Suzhou Nano Science and Technology. Financial supports from the National Natural Science Foundation of China (Grant nos. 11572309 and 11572310) and the National Basic Research Program of China (973 Program, Grant no. 2012CB937500) are gratefully acknowledged.

Appendix A. Supplementary material

Supplementary data associated with this article can be found in the online version at http://dx.doi.org/10.1016/j.jmmm.2016.02.005.

References

[1] C. Rinaldi, A. Chaves, S. Elborai, X. He, M. Zahn, Magnetic fluid rheology and flows, Curr. Opin. Colloid Interface Sci. 10 (2005) 141–157.
[2] S. Odenbach, Recent progress in magnetic fluid research, J. Phys.: Condens. Matter 16 (2004) R1135.
[3] R.E. Rosensweig, Heating magnetic fluid with alternating magnetic field, J. Magn. Magn. Mater. 252 (2002) 370–374.
[4] J. de Vicente, D.J. Klingenberg, R. Hidalgo-Alvarez, Magnetorheological fluids: a review, Soft Matter 7 (2011) 3701–3710.
[5] D. Li, H. Xu, X. He, H. Lan, Study on the magnetic fluid sealing for dry roots pump, J. Magn. Magn. Mater. 289 (2005) 419–422.
[6] R.M. Ferguson, K.R. Minard, K.M. Krishnan, Optimization of nanoparticle core size for magnetic particle imaging, J. Magn. Magn. Mater. 321 (2009) 1548–1551.
[7] G.J. Huang, B. Zhou, Z. Chen, H.H. Jiang, X.B. Xing, Magnetic-field sensor utilizing the ferrofluid and thin-core fiber modal interferometer, IEEE Sens. J. 15 (2015) 333–336.
[8] E. Brouzes, T. Kruse, R. Kimmerling, H.H. Strey, Rapid and continuous magnetic separation in droplet microfluidic devices, Lab Chip 15 (2015) 908–919.
[9] P. Li, D. Kilinc, Y.-F. Ran, G.U. Lee, Flow enhanced non-linear magnetophoretic separation of beads based on magnetic susceptibility, Lab Chip 13 (2013) 4400–4408.
[10] H. Rudolf, D. Silvio, Ml Robert, Z. Matthias, Magnetic particle hyperthermia: nanoparticle magnetism and materials development for cancer therapy, J. Phys.: Condens. Mat. 18 (2006) S2919.
[11] V. Skumryev, S. Stoyanov, Y. Zhang, G. Hadjipanayis, D. Givord, J. Nogues, Beating the superparamagnetic limit with exchange bias, Nature 423 (2003) 850–853.
[12] D.G. Shchukin, I.L. Radtchenko, G.B. Sukhorukov, Micron-scale hollow polyelectrolyte capsules with nanosized magnetic Fe_3O_4 inside, Mater. Lett. 57 (2003) 1743–1747.
[13] H. Chiriac, G. Stoian, Influence of the particles size and size distribution on the magnetorheological fluids properties, IEEE Trans. Magn. 45 (2009) 4049–4055.
[14] B.J. de Gans, N.J. Duin, D. van den Ende, J. Mellema, The influence of particle size on the magnetorheological properties of an inverse ferrofluid, J. Chem. Phys. 113 (2000) 2032–2042.

[15] J.M. Wang, J.F. Kang, Y.J. Zhang, X.J. Huang, Viscosity monitoring and control on oil-film bearing lubrication with ferrofluids, Tribol. Int. 75 (2014) 61–68.
[16] P. Berger, N.B. Adelman, K.J. Beckman, D.J. Campbell, A.B. Ellis, G.C. Lisensky, Preparation and properties of an aqueous ferrofluid, J. Chem. Educ. 76 (1999) 943.
[17] L.Q. Yu, L.J. Zheng, J.X. Yang, Study of preparation and properties on magnetization and stability for ferromagnetic fluids, Mater. Chem. Phys. 66 (2000) 6–9.
[18] H. Jung, H. Choi, Hydrothermal fabrication of octahedral-shaped Fe_3O_4 nanoparticles and their magnetorheological response, J. Appl. Phys. 117 (2015) 17E708.
[19] J.C. Love, A.R. Urbach, M.G. Prentiss, G.M. Whitesides, Three-dimensional self-assembly of metallic rods with submicron diameters using magnetic interactions, J. Am. Chem. Soc. 125 (2003) 12696–12697.
[20] K. Shah, J.S. Oh, S.B. Choi, R. Upadhyay, Plate-like iron particles based bidisperse magnetorheological fluid, J. Appl. Phys. 114 (2013) 213904.
[21] J. Dai, M. Yang, X. Li, H. Liu, X. Tong, Magnetic field sensor based on magnetic fluid clad etched fiber Bragg grating, Opt. Fiber. Technol. 17 (2011) 210–213.
[22] G. Salazar-Alvarez, J. Qin, V. Šepelák, I. Bergmann, M. Vasilakaki, K.N. Trohidou, J.D. Ardisson, W.A.A. Macedo, M. Mikhaylova, M. Muhammed, M.D. Baró, J. Nogués, Cubic versus spherical magnetic nanoparticles: the role of surface anisotropy, J. Am. Chem. Soc. 130 (2008) 13234–13239.
[23] M.-M. Song, W.-J. Song, H. Bi, J. Wang, W.-L. Wu, J. Sun, M. Yu, Cytotoxicity and cellular uptake of iron nanowires, Biomaterials 31 (2010) 1509–1517.
[24] K. Shah, S.B. Choi, The influence of particle size on the rheological properties of plate-like iron particle based magnetorheological fluids, Smart Mater. Struct. 24 (2015).
[25] N. Wereley, A. Chaudhuri, J.-H. Yoo, S. John, S. Kotha, A. Suggs, R. Radhakrishnan, B. Love, T. Sudarshan, Bidisperse magnetorheological fluids using Fe particles at nanometer and micron scale, J. Intell. Mater. Syst. Struct. 17 (2006) 393–401.
[26] R. Sheparovych, Y. Sahoo, M. Motornov, S. Wang, H. Luo, P.N. Prasad, I. Sokolov, S. Minko, Polyelectrolyte stabilized nanowires from Fe_3O_4 nanoparticles via magnetic field induced self-assembly, Chem. Mater. 18 (2006) 591–593.
[27] M. Johannsen, A. Jordan, R. Scholz, M. Koch, M. Lein, S. Deger, J. Roigas, K. Jung, S. Loening, Evaluation of magnetic fluid hyperthermia in a standard rat model of prostate cancer, J. Endourol. 18 (2004) 495–500.
[28] R.Y. Hong, T.T. Pan, H.Z. Li, Microwave synthesis of magnetic Fe_3O_4 nanoparticles used as a precursor of nanocomposites and ferrofluids, J. Magn. Magn. Mater. 303 (2006) 60–68.
[29] X. Ding, Z. Sun, W. Zhang, Y. Peng, A.S.C. Chan, P. Li, Characterization of Fe3O4/poly(styrene-co-N-isopropylacrylamide) magnetic particles with temperature sensitivity, Colloid Polym. Sci. 278 (2000) 459–463.
[30] J. Sun, S.B. Zhou, P. Hou, Y. Yang, J. Weng, X.H. Li, M.Y. Li, Synthesis and characterization of biocompatible Fe_3O_4 nanoparticles, J. Biomed. Mater. Res. A 80a (2007) 333–341.
[31] Z.H. Zhou, J. Wang, X. Liu, H.S.O. Chan, Synthesis of Fe_3O_4 nanoparticles from emulsions, J. Mater. Chem. 11 (2001) 1704–1709.
[32] V.P. Le, Q.H. Tran, T.S. Vo, S. Kim, J.H. Jeong, C. Kim, J.R. Jeong, Synthesis of monodisperse Fe_3O_4 nanoparticles by optimized sonochemical method using mono(Ethylene Glycol) (MEG), J. Nanosci. Nanotechnol. 11 (2011) 2726–2729.
[33] D.L. Huber, Synthesis, properties, and applications of iron nanoparticles, Small 1 (2005) 482–501.
[34] S. Xuan, F. Wang, Y.-X.J. Wang, J.C. Yu, K.C.-F. Leung, Facile synthesis of size-controllable monodispersed ferrite nanospheres, J. Mater. Chem. 20 (2010) 5086.
[35] C.F. Lee, M.L. Lin, Y.C. Wang, W.Y. Chiu, Synthesis and characteristics of poly (N-isopropylacrylamide-co-methacrylic acid)/Fe_3O_4 thermosensitive magnetic composite hollow latex particles, J. Polym. Sci. Part A: Polym. Chem. 50 (2012) 2626–2634.
[36] F.F. Fang, H.J. Choi, M.S. Jhon, Magnetorheology of soft magnetic carbonyl iron suspension with single-walled carbon nanotube additive and its yield stress scaling function, Colloids Surf. A 351 (2009) 46–51.
[37] K. Shah, R.V. Upadhyay, V.K. Aswal, Influence of large size magnetic particles on the magneto-viscous properties of ferrofluid, Smart Mater. Struct. 21 (2012) 075005.
[38] A.P. Philipse, D. Maas, Magnetic colloids from magnetotactic bacteria: chain formation and colloidal stability, Langmuir 18 (2002) 9977–9984.
[39] P. Ilg, M. Kröger, S. Hess, Magnetoviscosity of semidilute ferrofluids and the role of dipolar interactions: comparison of molecular simulations and dynamical mean-field theory, Phys. Rev. E 71 (2005) 031205.
[40] B.-J. Gans, Non-linear magnetorheological behaviour of an inverse ferrofluid, Faraday Discuss. 112 (1999) 209–224.
[41] M. Mohebi, N. Jamasbi, J. Liu, Simulation of the formation of nonequilibrium structures in magnetorheological fluids subject to an external magnetic field, Phys. Rev. E 54 (1996) 5407.
[42] A. Satoh, G.N. Coverdale, R.W. Chantrell, Stokesian dynamics simulations of ferromagnetic colloidal dispersions subjected to a sinusoidal shear flow, J. Colloid Interface Sci. 231 (2000) 238–246.
[43] G.M. Whitesides, The origins and the future of microfluidics, Nature 442 (2006) 368–373.